J. Phys. B: Atom. Molec. Phys., Vol. 11, No. 22, 1978. Printed in Great Britain

Differential and integral cross sections for the electron impact excitation of O_2 II. Optically forbidden transitions from the ground state

K Wakiya
Department of Physics, Faculty of Science and Technology, Sophia University, Chiyoda-ku, Tokyo 102, Japan

Received 8 March 1978, in final form 26 June 1978

Abstract. The electron impact excitation spectrum of O_2 has been studied for the scattering angle range from 10 to 130° and the energy-loss range from 0 to 7·1 eV. Differential and integral cross sections for excitation of the a $^1\Delta_g$ and b $^1\Sigma_g^+$ states and a group of states ranging from about 4·5 to 7·1 eV energy loss (broad maximum at 6·1 eV) have been determined in the impact energy ranges E_0 = 20–200 eV, 20–150 eV and 20–500 eV, respectively. They are the first experimental data on the cross sections for excitation of these states at collision energies larger than 50 eV. The 6·1 eV broad peak is designated as the sum of the excitation to the A $^3\Sigma_u^+$, C $^3\Delta_u$ and c $^1\Sigma_u^-$ states by virtue of the angular distribution and energy dependence of the differential and integral cross sections.

1. Introduction

Molecular oxygen is a key element in life and plays an important role in science and technology. The a $^1\Delta_g$ and b $^1\Sigma_g^+$ states are of considerable interest in the chemistry of excited states and in upper atmosphere studies. However, very few measurements of their electron impact excitation have been reported.

Schulz and Dowell (1962) determined upper limits on the integral cross sections for excitation of the a $^1\Delta_g$ and b $^1\Sigma_g^+$ states of 3×10^{-20} and 6×10^{-21} cm^2, respectively, at 0·16 eV above threshold using the trapped-electron method. Skerbele *et al* (1968) found that the relative intensity of the a $^1\Delta_g$ state referred to the elastic peak remained constant ($1{\cdot}3 \times 10^{-4}$) in the scattering angle range 3–12° at E_0 = 45 eV. Konishi *et al* (1970) measured integral cross sections for excitation of the a $^1\Delta_g$ and b $^1\Sigma_g^+$ states in the impact energy range at E_0 = 20–70 eV. Trajmar *et al* (1971, 1972) measured the differential and integral cross sections for excitation of the a $^1\Delta_g$ and b $^1\Sigma_g^+$ states for energies E_0 = 4–45 eV and scattering angles θ = 10–90°. At E_0 = 20 and 45 eV, they also measured the broad peak which has a maximum around 6·1 eV energy loss. This excitation energy covers the A $^3\Sigma_u^+$, C $^3\Delta_u$ and c $^1\Sigma_u^-$ states (A $^3\Sigma_u^+$ + C $^3\Delta_u$ + c $^1\Sigma_u^-$), but Trajmar *et al* assigned this peak to be mostly due to the excitation of the c $^1\Sigma_u^-$ state.

For inelastic electron–molecule scattering Cartwright *et al* (1971) found the rigorous selection rule that the differential cross section (DCS) for a $\Sigma^+ \leftrightarrow \Sigma^-$ transition is identically zero at 0 and 180° scattering angles. Hall and Trajmar (1975) determined differential and integral cross sections for scattering of 4·5 eV electrons by oxygen molecules in the ground (x $^3\Sigma_g^-$) state and the metastable (a $^1\Delta_g$) state.

Experimental differential and integral cross sections for electron impact excitation of the a $^1\Delta_g$, b $^1\Sigma_g^+$ and (A $^3\Sigma_u^+$ + c $^3\Delta_u$ + c $^1\Sigma_u^-$) states are reported here for incident energies from 20 to 500 eV and scattering angles from 10 to 130°.

2. Experimental results

2.1. *Differential cross section*

The apparatus used in the present study is identical to that described in a previous paper (Wakiya 1978).

A typical electron impact energy-loss spectrum of O_2 is shown in figure 1. Excitation of the Schumann–Runge continuum and the electronic states ranging from 9·7 to 12·1 eV of energy loss have been reported earlier by Wakiya (1978). In the energy-loss region below the Schumann–Runge continuum in the spectrum in figure 1, we can see two sharp peaks and one broad peak at 0·98, 1·63 and at about 6·1 eV, respectively. The first two peaks are assigned to the excitation of the infrared atmospheric band (a $^1\Delta_g \leftarrow$ x $^3\Sigma_g^-$) and the atmospheric band (b $^1\Sigma_g^+ \leftarrow$ x $^3\Sigma_g^-$), respectively. Each of the energy-loss structures for excitation of the a $^1\Delta_g$ and b $^1\Sigma_g^+$ states consists of a single peak which can be assigned to the $v' = 0 \leftarrow v'' = 0$ transition from the ground electronic state. This is reasonably understood from the fact that the bottoms of the potential energy curves of these states are situated at approximately the same internuclear distance as the ground state, and that the shape of the potential curves is also very similar to that of the ground state. Therefore the Franck–Condon region from the ground state is just within the range where the overlap integral is concentrated in the $v' = 0$ vibrational level.

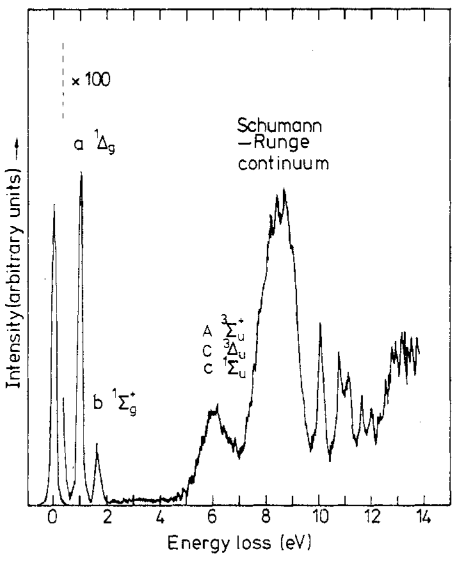

Figure 1. Electron impact energy-loss spectrum of O_2. Impact energy E_0 = 70 eV. Scattering angle θ = 90°. Energy-loss region 0–13·8 eV.

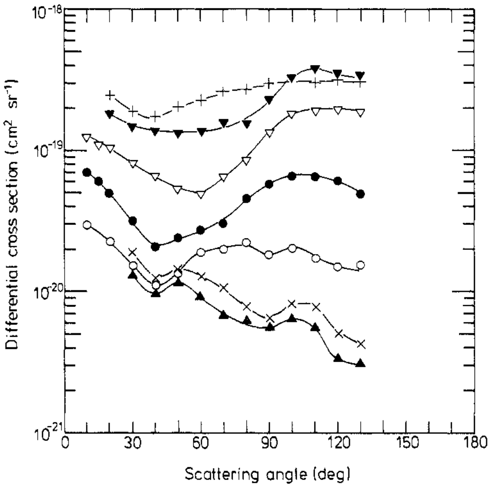

Figure 2. The DCS for the a $^1\Delta_g \leftarrow$ X $^3\Sigma_g^-$ excitation in O_2 for different incident electron energies: + 20 eV, ▼ 30 eV, ▽ 50 eV, ● 70 eV, ○ 100 eV, × 150 eV, ▲ 200 eV.

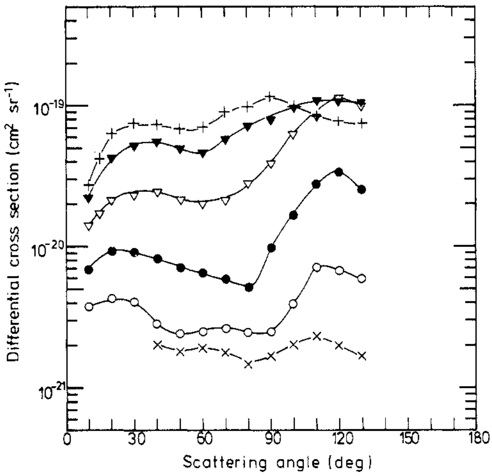

Figure 3. The DCS for the b $^1\Sigma_g^+ \leftarrow$ X $^3\Sigma_g^-$ excitation in O_2 for different incident electron energies: + 20 eV, ▼ 30 eV, ▽ 50 eV, ● 70 eV, ○ 100 eV, × 150 eV.

A broad peak, which has a maximum around 6·1 eV and ranges from 4·5 to 7·1 eV energy loss, covers the excitations of the electronic states A $^3\Sigma_u^+$, C $^3\Delta_u$ and c $^1\Sigma_u^-$. For transitions to these electronic states from the ground state, the Franck–Condon region is in the continuum, and these cannot be resolved. It depends on the impact energy and the scattering angle, as discussed later, to which state of the three the excitation is most prominent.

The DCS for excitation of the a $^1\Delta_g$, b $^1\Sigma_g^+$ and (A $^3\Sigma_u^+$ + C $^3\Delta_u$ + c $^1\Sigma_u^-$) states from the ground state are shown in figures 2, 3, 4(*a*) and (*b*), respectively, as functions of the scattering angle.

The following features in the angular and energy dependences of the DCS are seen from these figures.

(i) The DCS decrease as the impact energy E_0 increases except for $\theta < 30°$ in figure 4(*a*).

(ii) The DCS show nearly isotropic behaviour for low impact energies (below 50 eV) except for $\theta < 30°$ of figure 3. This suggests that these transitions are mainly due to electron exchange.

(iii) The DCS for all the states have a shallow minimum around the following scattering angles:

a $^1\Delta_g$ state	$\theta = 40\text{–}60°$	($E_0 = 50\text{–}200$ eV)
b $^1\Sigma_g^+$ state	$\theta = 60\text{–}80°$	($E_0 = 20\text{–}150$ eV)
(A $^3\Sigma_u^+$ + C $^3\Delta_u$ + c $^1\Sigma_u^-$) states	$\theta = 60\text{–}80°$	($E_0 = 70\text{–}200$ eV).

From comparison between figure 2 and figure 4(*a*), the following features can be pointed out.

(i) The DCS for the (A $^3\Sigma_u^+$ + C $^3\Delta_u$ + c $^1\Sigma_u^-$) states show an angular dependence very similar to that for the a $^1\Delta_g$ state in the energy range below $E_0 = 100$ eV. This implies that the 6·1 eV broad peak is dominated mostly by the electron exchange process (c $^1\Sigma_u^- \leftarrow$ X $^3\Sigma_g^-$) at $E_0 < 100$ eV. This interpretation is supported by the energy dependence of the integral cross section (see §2.2).

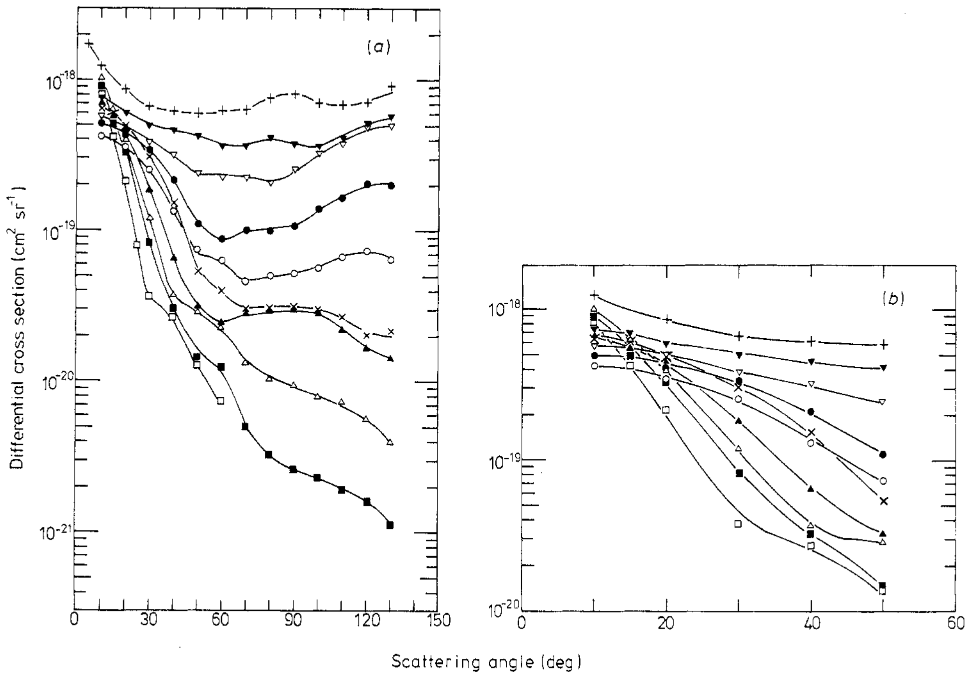

Figure 4. (*a*) The DCS for the (A $^3\Sigma_u^-$ + c $^3\Delta_u$ + c $^1\Sigma_u^-$) $\leftarrow$ X $^3\Sigma_g^-$ excitation in O_2 for different incident electron energies: + 20 eV, ▼ 30 eV, ▽ 50 eV, ● 70 eV, ○ 100 eV, × 150 eV, ▲ 200 eV, △ 300 eV, ■ 400 eV, □ 500 eV. (*b*) As (*a*), except that the scale of scattering angle is extended three times in the range of $\theta = 10$–$50°$.

(ii) For the high incident energies used in this study, the angular dependence of the DCS for excitation of the (A $^3\Sigma_u^+$ + c $^3\Delta_u$ + c $^1\Sigma_u^-$) states appears to peak in the forward direction. This tendency becomes remarkably stronger for $E_0 > 100$ eV. This suggests that excitations of the (A $^3\Sigma_u^+$ + c $^3\Delta_u$ + c $^1\Sigma_u$) states are dominated mostly by the direct scattering process.

Figure 3 shows that the DCS falls off at small and large scattering angles. This behaviour of the DCS is in agreement with the selection rule for a $\Sigma^+ \leftrightarrow \Sigma^-$ transition that the DCS must be zero at scattering angles of 0 and 180° (Cartwright *et al* 1971).

Very recently Cartwright *et al* (1977) reported that the DCS for the B′ $^3\Sigma_u^-$ and a′ $^1\Sigma_u^-$ states in N_2 show a fall off at small and large scattering angles. Furthermore, the angular dependence of the DCS in figure 3 shows a well pronounced double-peaked shape, where the peak at smaller scattering angles is generally smaller than that at larger scattering angles.

The present DCS results for excitation of the (A $^3\Sigma_u^+$ + c $^3\Delta_u$ + c $^1\Sigma_u^-$), a $^1\Delta_g$ and b $^1\Sigma_g^+$ states are compared in figure 5 and figure 6 with the results of Trajmar *et al* (1971, 1972). Although the magnitudes of the DCS agree within the experimental error and the angular distributions agree fairly well, the present DCS are smaller than the results of Trajmar *et al* on the whole. This difference is thought to be mainly due to the difference in the elastic DCS used as the standard for normalisation to an absolute scale (see Wakiya 1978, §4.2.4). In the case of figure 6, the impact energy used by Trajmar *et al* is smaller by 5 eV than the present one, which accounts for the slight difference between the DCS.

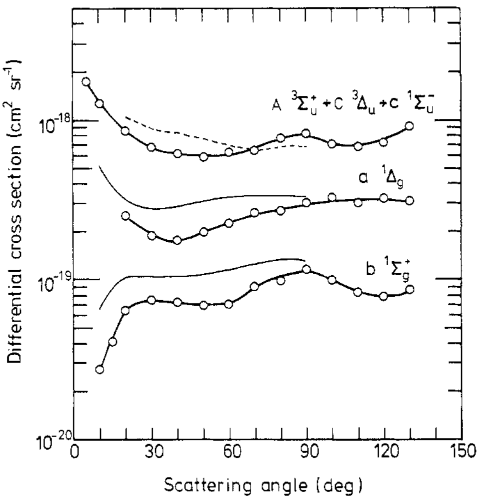

Figure 5. The DCS for excitation of the (A $^3\Sigma_u^+$ + c $^3\Delta_u$ + c $^1\Sigma_u^-$), a $^1\Delta_g$ and b $^1\Sigma_g^+$ states in O_2 at an impact electron energy of E_0 = 20 eV. The symbols ○ and the bold curves show the present results. The broken curve (A $^3\Sigma_u^+$ + c $^3\Delta_u$ + c $^1\Sigma_u^-$) and the fine curve (a $^1\Delta_g$ and b $^1\Sigma_g^+$) indicate the measured values of Trajmar *et al* (1972, 1971), respectively.

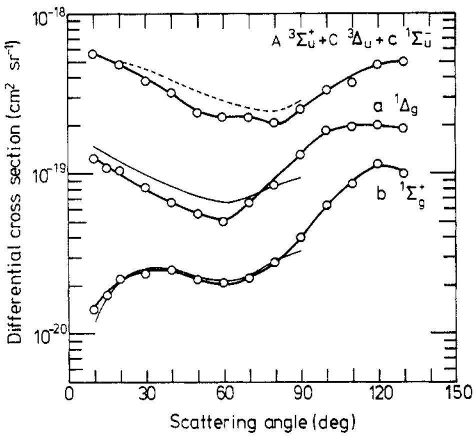

Figure 6. Same as figure 5, except for impact electron energies E_0 = 50 eV (present results) and E_0 = 45 eV (results of Trajmar *et al*; the broken curve and fine curve).

Although a comparison of the present data with theoretical calculations is desirable, it could not be made because up to now no theoretical calculations are available for these inelastic scattering processes in O_2.

2.2. *Integral cross section*

In figure 7 integral cross sections for excitation of the (A $^3\Sigma_u^+$ + c $^3\Delta_u$ + c $^1\Sigma_u^-$), a $^1\Delta_g$ and b $^1\Sigma_g^+$ states are shown as a function of the impact energy E_0. Cross sections for excitation of respective states are marked as σ_{ACc}, σ_a and σ_b. The measured values by Trajmar *et al* (1971, 1972) and Linder *et al* (1971) are also shown in figure 7 for comparison.

We estimate the overall uncertainty in the cross section determinations to be 40% for the collision energies smaller than 50 eV, and 50% for higher energies.

From a comparison of integral cross sections σ_{ACc}, σ_a and σ_b in figure 7, the following features are pointed out.

(i) The relation between the magnitudes of these integral cross sections is $\sigma_{ACc} > \sigma_a > \sigma_b$, which is independent of the electron impact energy E_0. For E_0 = 20–150 eV, σ_{ACc}/σ_a = 3–8, σ_a/σ_b = 3–5.

(ii) The present cross sections σ_{ACc}, σ_a and σ_b decrease as the impact energy increases from 20 eV. For example, $\sigma_a(150\ \mathrm{eV})/\sigma_a(20\ \mathrm{eV}) = 3{\cdot}5 \times 10^{-2}$, $\sigma_b(150\ \mathrm{eV})/\sigma_b(20\ \mathrm{eV}) = 2{\cdot}3 \times 10^{-2}$, $\sigma_{ACc}(500\ \mathrm{eV})/\sigma_{ACc}(20\ \mathrm{eV}) = 3{\cdot}2 \times 10^{-2}$.

(iii) For the impact energy range E_0 = 50–100 eV we found that the cross sections σ_{ACc}, σ_a and σ_b decrease approximately as $E_0^{-2{\cdot}7}$, $E_0^{-2{\cdot}9}$ and $E_0^{-3{\cdot}1}$, respectively. This energy dependence in the integral cross section shows reasonable agreement with the theoretical prediction of E_0^{-3} in the electron-exchange collision by Ochkur *et*

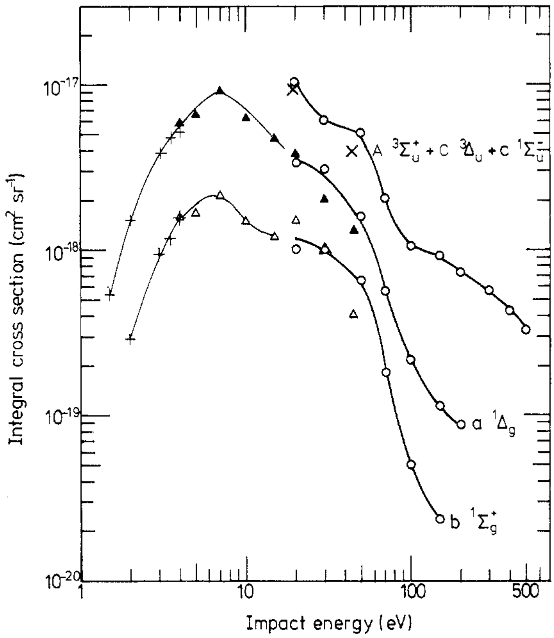

Figure 7. Integral cross sections for excitation of the (A $^3\Sigma_u^+$ + c $^3\Delta_u$ + c $^1\Sigma_u^-$), a $^1\Delta_g$ and b $^1\Sigma_g^+$ states of O_2 as a function of electron impact energy. The symbols ○ and the bold curves show the present data. The symbols × (A $^3\Sigma_u^+$ + c $^3\Delta_u$ + c $^1\Sigma_u^-$), ▲ (a $^1\Delta_g$) and △ (b $^1\Sigma_g^+$) indicate the results of Trajmar *et al* (1971, 1972). The symbols + indicate the results of Linder and Schmidt (1971) for the a $^1\Delta_g$ and b $^1\Sigma_g^+$ states.

al (1965). At these impact energies, it is suggested that transitions from the ground state to the (A $^3\Sigma_u^+$ + c $^3\Delta_u$ + c $^1\Sigma_u^-$), a $^1\Delta_g$ and b $^1\Sigma_g^+$ states occur mostly via the electron-exchange process.

(iv) For E_0 = 100–500 eV, σ_{ACc} decreases as $E_0^{-0\cdot 9}$. Integral cross sections for the symmetry-forbidden transition are known to be given by Bethe theory, and decrease as E_0^{-1} when the energy of the incident electron is sufficiently high (Inokuti 1971). The cross section σ_{ACc} appears to behave in this manner in the high-energy region. A bend point is seen in the curve of energy dependence for σ_{ACc} at about E_0 = 100 eV. This bend is thought to originate from the change of the transition mechanism, that is, the direct excitation process takes the place of the electron-exchange process as the incident electron energy increases.

3. Discussion

The transitions a $^1\Delta_g \leftarrow$ X $^3\Sigma_g^-$ and b $^1\Sigma_g^+ \leftarrow$ X $^3\Sigma_g^-$ are optically forbidden. The former involves the change of angular momentum $\Delta\Lambda = 2$, the change of spin $\Delta S = 1$ and a transition between the two g (even) states; the latter similarly involves $\Delta S = 1$, $\Sigma^+ \leftarrow \Sigma^-$ (reflection symmetry forbidden) and g $\leftarrow$ g, which are all in conflict with the selection rules for the electric dipole transition. The selection rules $\Delta\Lambda = 0, \pm 1$, $\Delta S = 0$ and $\Sigma^- \leftrightarrow \Sigma^-$ are often broken due to the effects of spin–orbit interaction, but the rule g $\not\leftrightarrow$ g is never broken. In reality, the above transitions are observed in optical spectra and they are known to be caused by the magnetic dipole interaction (Herzberg 1969, pp 147–9, Garstang 1962).

The ($A\,^3\Sigma_u^+ - X\,^3\Sigma_g^-$), ($c\,^1\Sigma_u^- - X\,^3\Sigma_g^-$) and ($C\,^3\Delta_u$–$X\,^3\Sigma_g^-$) transitions are called Herzberg I, II and III systems, respectively. They were identified by the systematic absorption measurements by Herzberg (1932, 1952, 1953). These transitions are also optically forbidden, since the first one involves the transition $\Sigma^+ \leftrightarrow \Sigma^-$, the second one $\Delta S = 1$ and the last one $\Delta\Lambda = 2$, respectively, which are all in conflict with the selection rules for electric dipole transition. As spin–orbit coupling exists, these transitions are observed in optical spectra, and they are known to occur by the electric dipole interaction since the most rigorous rule of $u \leftrightarrow g$ is fulfilled (Herzberg 1969, p 147, Krupenie 1972, pp 431–3).

On the other hand, on the basis of the present measurement of the angular and energy dependences of the DCS, and quantitative consideration of the energy dependence of integral cross sections, the properties of these transitions are characterised by the following mechanism in the case of electron impact.

The transitions $a\,^1\Delta_g \leftarrow X\,^3\Sigma_g^-$ and $b\,^1\Sigma_g^+ \leftarrow X\,^3\Sigma_g^-$ are interpreted to be caused by the electron exchange mechanism.

The major part of σ_{ACc} comes from the transition $c\,^1\Sigma_u^- \leftarrow X\,^3\Sigma_g^-$ for low collision energies ($E_0 < 100$ eV) and this is also caused by the electron exchange mechanism.

However for high collision energies ($E_0 > 100$ eV) the major part of σ_{ACc} can be said to come from the transitions $A\,^3\Sigma_u^+ \leftarrow X\,^3\Sigma_g^-$ and $C\,^3\Delta_u \leftarrow X\,^3\Sigma_g^-$, and these are caused by the direct scattering mechanism.

Trajmar *et al* (1972) assigned the excitation of the 6·1 eV broad peak as coming from the ($c\,^1\Sigma_u^- \leftarrow X\,^3\Sigma_g^-$) transition on the basis of the angular distribution of DCS in their experiments at $E_0 = 20$ and 45 eV. For the low impact energy region, the assignments by Trajmar *et al* agree with the present ones.

The integral cross sections σ_a and σ_b obey approximately the E_0^{-3} dependence, in accordance with the Ochkur approximation, for $E_0 > 50$ eV. The σ_c is also considered to show the same energy dependence for $E_0 > 50$ eV.

σ_{AC} is considered to show the E_0^{-1} dependence, in accordance with the Bethe approximation, for $E_0 > 100$ eV. Here, σ_c and σ_{AC} represent the integral cross sections for the $c\,^1\Sigma_g^- \leftarrow X\,^3\Sigma_g^-$ and ($A\,^3\Sigma_u^+ + C\,^3\Delta_u$) $\leftarrow X\,^3\Sigma_g^-$ transitions, respectively, and so $\sigma_{ACc} = \sigma_{AC} + \sigma_c$.

Acknowledgments

The author is grateful to Professor H Suzuki, Dr T Takayanagi, Professor S Yoshida, Professor Y Kaneko and Dr I Shimamura for stimulating discussions and criticising the manuscript. He is also indebted to Messrs A Yagishita, H Oomoto, A Nakashio and Miss C Hirota for their help in the measurement of the experimental data.

References

Cartwright D C, Trajmar S, Chutjian A and Williams W 1977 *Phys. Rev.* A **16** 1013–40
Cartwright D C, Trajmar S, Williams W and Huestis D L 1971 *Phys. Rev. Lett.* **27** 704–7
Garstang R H 1962 *Atomic and Molecular Processes* ed D R Bates (New York and London: Academic Press) pp 1–46

Hall R I and Trajmar S 1975 *J. Phys. B: Atom. Molec. Phys.* **8** L293–6
Herzberg G 1932 *Naturwiss.* **20** 577
——1952 *Can. J. Phys.* **30** 185–210
——1953 *Can. J. Phys.* **31** 657–69
——1969 *Mem. Soc. R. Sci. Liege Collect.* **17** 121–55
Inokuti M 1971 *Rev. Mod. Phys.* **43** 297–347
Konishi A, Wakiya K, Yamamoto M and Suzuki H 1970 *J. Phys. Soc. Japan* **29** 526
Krupenie P H 1972 *J. Phys. Chem. Ref. Data* **1** 423–534
Linder F and Schmidt H 1971 *Z. Naturf.* **26** 1617–25
Ochkur V I and Brattsev V F 1965 *Opt. Spectrosc.* **19** 274
Schulz G J and Dowell J T 1962 *Phys. Rev.* **128** 174–7
Skerbele A, Dillon M A and Lassettre E N 1968 *J. Chem. Phys.* **49** 3542–5
Trajmar S, Cartwright D C and Williams W 1971 *Phys. Rev.* A **4** 1482–92
Trajmar S, Williams W and Kuppermann A 1972 *J. Chem. Phys.* **56** 3759–65
Wakiya K 1978 *J. Phys. B: Atom. Molec. Phys.* **11** 3913–30